29 Ring Laser Gyroscopes as Rotation Sensors for Seismic Wave Studies

K. Ulrich Schreiber[1], Geoffrey E. Stedman[2], Heiner Igel[3], Asher Flaws[3]

[1]Forschungseinrichtung Satellitengeodäsie der TU- München,
Arcisstr. 21, 80333 München, Germany
e-mail: schreiber@wettzell.ifag.de

[2]Department of Physics and Astronomy,
University of Canterbury, Private Bag 4800, New Zealand
e-mail: geoffrey.stedman@canterbury.ac.nz

[3]Department für Geo- und Umweltwissenschaften, Sektion Geophysik,
Ludwig-Maximilians-Universität München,
Theresienstr. 41, 80333 München, Germany
e-mail: heiner.igel@geophysik.uni-muenchen.de

29.1 Introduction

Although their importance was understood (Aki and Richards 2002), rotations have long been neglected in seismic studies because no suitable sensors existed. The technology for seismometers exploiting the inertia of a test mass, on the other hand, is well established and such sensors are nowadays sensitive, reliable and reasonably cheap. In general, there is a variety of different concepts for rotation sensors available, such as a pendulum, micromechanic tuning fork gyros, fiber optic gyros and ring lasers. The latter, when scaled up, have the advantage of an extremely high sensitivity.

Over the last 40 years, ring laser gyroscopes have become one of the most important instruments in the field of inertial navigation and precise rotation measurements. They have a high resolution, good stability and a wide dynamic range. Furthermore, no spinning mechanical parts are required, so these sensors can be manufactured in a very robust way. These properties made them very suitable for aircraft navigation. For more than 10 years, very large perimeter ring laser gyroscopes have been specifically developed for applications in geodesy and geophysics (Schreiber et al.

2001). By increasing the effective ring laser area by up to a factor of 24,000 over the size of an aircraft gyro, the sensitivity of these ring lasers to rotation has improved by at least 5 orders of magnitude, while the drift rate of the instruments has been reduced substantially. With several of these highly stable large ring lasers, very small periodic signals coming from polar motion, solid Earth tides and ocean loading have been successfully measured (Schreiber et al. 2003, 2004a). However, rotational signal signatures caused by remote earthquakes are stronger than these small perturbations of Earth rotation (McLeod et al. 1998, Pancha et al. 2000). The range of angular velocities to be covered is very wide: 10^{-14} rad/s $\leq \Omega_s \leq$ 1 rad/s, with the required frequency bandwidth for the seismic waves in the range of 3 mHz $\leq f_s \leq$ 10 Hz (Schreiber et al. 2004b). Currently, the large ring lasers are the only available rotation sensors which fulfil these demands. Three such devices mounted in orthogonal orientations may eventually provide the quantitative detection of rotations from shear, Love and Rayleigh waves. These properties inspired the development of a highly sensitive ring laser gyro dedicated to seismological applications. It is important to note that ring laser gyroscopes are sensitive only to rotations around their area normal vector. From that point of view, they provide additional information.

The goal of the GEOsensor project was the construction and evaluation of a field-deployable demonstrator unit, which will eventually provide access to all 6 degrees of freedom of motion. The recording of the (complete) earthquake-induced rotational motion is expected to be particularly useful for: (1) further constraining earthquake source processes when observed close to the active faults (Takeo and Ito 1997); (2) estimating permanent displacement from seismic recordings (Trifunac and Todorovska 2001); (3) estimating local (horizontal) phase velocities from collocated observations of translations and rotations (Igel et al. 2005). Because of the relatively short duration of an earthquake, such ring lasers do not need a long term stability over weeks or months, which is difficult and expensive to obtain. An instrumental stability of approximately one hour during a seismic event is sufficient. Therefore it is possible to use a steel structure attached to a solid concrete platform as the main components of the Sagnac interferometer. As indicated above, ring lasers for seismic studies require a high data rate of at least 20 Hz, because of the wide bandwidth of seismic frequencies near an earthquake source. While large ring lasers for geodetic applications are usually optimized for measuring variations in the rotation rate of the Earth in a frequency band below 1 mHz, autoregressive algorithms can be used to determine the Sagnac frequency with a resolution below the Nyquist limit. While this method can still be employed for the strongly bandwidth limited teleseismic signals (McLeod et al. 2001), an

entirely different detection scheme is needed for the data evaluation of regional or local seismic events.

29.2 Properties of Ring Lasers

Ring lasers are active Sagnac interferometers, where two monomode laser beams circulate around a triangular or square closed cavity in opposite directions (Aronowitz 1971, Stedman 1997). If the whole apparatus is placed on a platform rotating with respect to inertial space, the effective cavity length differs between the co-rotating and the anti-rotating laser beams and one obtains a frequency splitting of the two counter propagating optical waves, the magnitude of which is directly proportional to the rate of rotation. The Sagnac frequency δf is

$$\delta f = \frac{4A}{\lambda P}\,\mathbf{n}\cdot\Omega\,, \tag{29.1}$$

where A is the area, P is the perimeter enclosed by the beam path and λ is the optical wavelength of the laser oscillation. Ω is the angular velocity at which the instrument is turning and $\mathbf{n}$ is the normal vector to the laser beam plane. In order to understand the functions of such a Sagnac interferometer with respect to applications in seismology, one can distinguish three independent mechanisms contributing to the measured beat frequency δf. These are: scale factor $4A/\lambda P$, orientation $\mathbf{n}\cdot\Omega$, and rotation velocity $\Omega(t)$.

29.2.1 Scale factor

A number of helium/neon ring lasers with square resonators have been successfully constructed over the last 15 years. Basic design features common to all of them are laser cavities with an extremely high Q around 10^{12} ($Q = \omega\,\tau$, with ω the optical frequency and τ the cavity decay time) and a rf-plasma excitation scheme. All these ring lasers are operated near laser threshold, using mode competition as a natural selection criterion to ensure single longitudinal mode operation for each sense of rotation (Stedman 1997). The lock-in threshold is well below 1 Hz; therefore, all of these rings are always unlocked at the rate bias generated from the rotating Earth. From Eq. (29.1) one can see that the geometrical stability of the ring laser cavity is very important, because small variations in the scale factor impact on the Sagnac frequency. For relatively small ring lasers, which can

be manufactured from a monolithic Zerodur body such as C-II (A = 1 m^2) and G (A = 16 m^2), it is possible to fulfil this condition. However, for very large ring lasers, namely UG1 (A = 367 m^2) and UG2 (A = 832 m^2) it is impossible to keep the scale factor constant. These instruments are made from stainless steel tubes mounted on small concrete piers inside the Cashmere Cavern in Christchurch, New Zealand. Apart from distortions of the cave caused by changes in temperature and atmospheric pressure, such a ring laser is also exposed to a variable strain field induced by the gravitational forces of the moon.

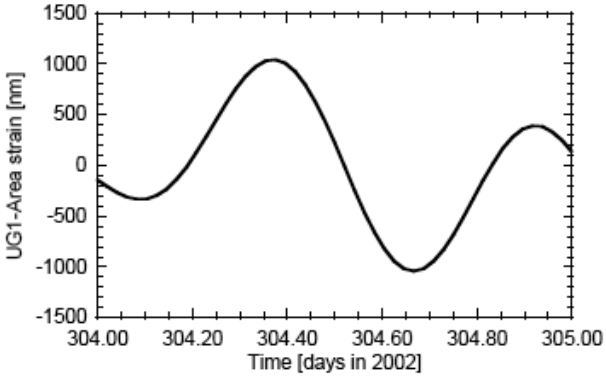

Fig. 29.1 Area strain for the UG1 ring laser location computed from global model for the day 304 in 2002. The maximum peak to peak variation of the perimeter is around 2.5 μm

Figure 29.1 shows an example for the modelled area strain acting on the UG1 ring laser. The perimeter changes by as much as 2.5 μm as a result of the deformation of the Earth crust caused by lunar attraction. However this is not the only effect. Atmospheric pressure changes also cause deformations to the Cashmere cavern. A way to analyse these variations of the ring laser perimeter is to operate the ring laser in two neighbouring longitudinal modes and the measurement of the resultant beat frequency, which corresponds to the free spectral range (FSR) of the cavity. The FSR is defined as FSR = C/P and when measured can be used to determine the perimeter (P) of the ring laser accurately. For the UG1 ring laser the FSR is 3.8969041 MHz. In order to allow a detailed study of the variation of the cavity length this rf-signal was downconverted to an audio signal of around 282 Hz with a help of a GPS-stabilized signal generator. Figure 29.2 shows the result.

Good agreement has been obtained between model and measurement. Since the atmospheric pressure constantly dropped over the time of the measurement, it was included into the analysis as a linear drift. As a result

of this investigation one can conclude that it is impossible to keep the perimeter and therefore the scale factor constant for very large rings.

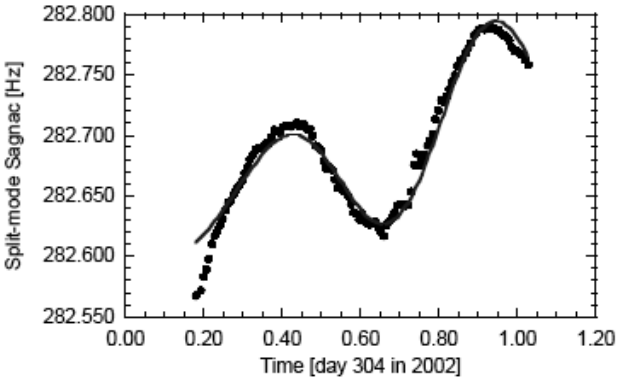

Fig. 29.2 Area strain for the UG1 ring laser location computed from a global model extended with a linear drift from atmospheric pressure changes (solid curve) superimposed on FSR measurements of the ring laser cavity (dotted curve)

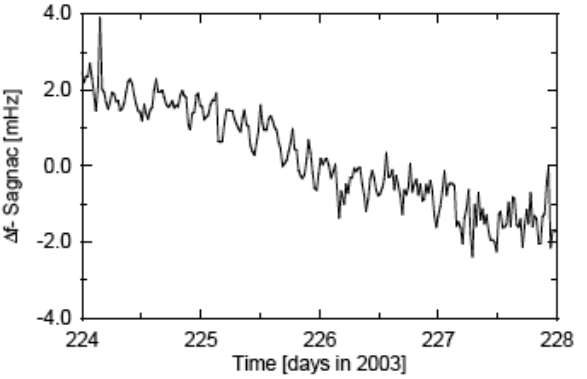

Fig. 29.3 Example of a timeseries of the Sagnac frequency variations from UG1. here is a general sensor drift apparent, but strain related scale factor changes are not present

Figure 29.3 shows an arbitrary example of a longer timeseries of Earth rotation measurements from the UG1 ring laser. One can see that there are no apparent contributions of the scale factor variations in this dataset. Since Fig. 29.3 has a measurement resolution of approx. 1 ppm (part per million) of the measurement quantity, this is surprising. According to the ring laser equation, Eq. 29.1, the scaling factor is depending on the perimeter and area. The wavelength of the laser is given by

$$\lambda = \frac{P}{I}, \tag{29.2}$$

where P is the perimeter and I the index of the longitudinal mode. For a square cavity and under the assumption that any change in area also reflects in the corresponding change of the perimeter (that is, in the absence of distortions of the ring laser), one finds that the scaling factor is independent of the wavelength and the ring laser dimensions as long as the same longitudinal index of the laser mode is maintained. The Sagnac formula then can be written as

$$\delta f = \frac{4IA}{P^2}\mathrm{n}\cdot\Omega, \tag{29.3}$$

For an exact square cavity, where one side is a, the scale factor reduces to $I/4$. Since area and perimeter changes correspond to each other in general, this means that the scale factor variations of this type do not appear in the Sagnac frequency as long as the longitudinal mode index does not change. This is usually the case. As the area changes, the perimeter and the instantaneous optical frequency inside the laser cavity will respond to compensate for the changes. This means, the large ring lasers are suitable instruments for seismic studies.

29.2.2 Ring laser orientation

Because of the inner product in Eq. 29.1, the value of the measurement quantity also depends on the projection of the rotation vector on the ring laser normal vector. Geophysical signals such as the solid Earth tides, ocean loading and diurnal polar motion become measurable via the variation of this projection (Schreiber et al. 2003, 2004a). Therefore, it is also important to look at this effect for the interpretation of seismic wave detections. Figure 29.4 gives an example of a $M = 6.8$ earthquake that occurred in Algeria on May 21 in 2003. It was recorded at the G ring laser facility of the geodetic observatory Wettzell in Southern Germany.

The upper part of the diagram shows the Sagnac frequency converted to a rotation rate as measured during the earthquake. The lower part of the diagram was obtained by taking the simultaneously recorded tiltmeter readings (referenced to local g) and converting them to a projection-induced variation of the rotation rate. In comparison, one can see that this tilt signal contributes less than 5% to the total signal. For an earthquake with a large epicentral distance, this effect is smaller, but for much closer earthquakes it may well become a dominant signal source. This again

shows how important it will be to measure all 6 degrees of freedom of motion close to an earthquake source.

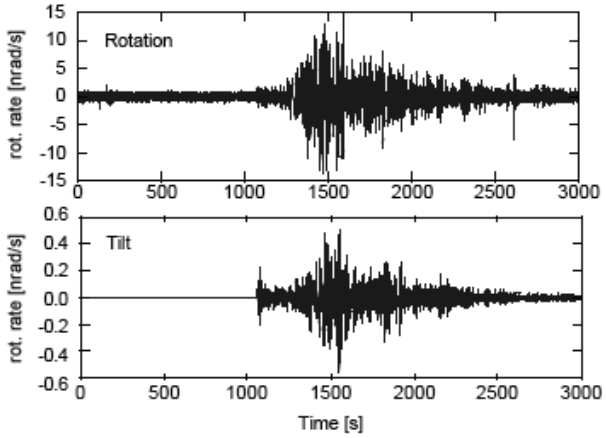

Fig. 29.4 Ring laser seismogram of an earthquake in Algeria ($M = 6.8$) of 21 May 2003, recorded by the G ring laser in Wettzell. The tilt induced contribution to the measurement quantity is as large as 5%

29.2.3 Instrumental dynamic range

Unlike seismometers, the concept of a Sagnac interferometer is not based on mass inertia. As a consequence, ring lasers have no moving mechanical parts. This has the advantage that there is no restitution process required for the extraction of the true ground motion from the transfer function of the measurement device. In order to distinguish true measured ground rotations from possible unknown sensor artefacts, two independent ring lasers were co-located and operated at the same place. The first ring laser is C-II, a monolithic solid body structure with an effective area of 1 m^2, the second ring is the heterogeneous UG1, built on many small independent concrete pedestals around the inner perimeter of the Cashmere cave. UG1 has an effective area of 467 m^2. C-II is placed inside UG1 and the area normal vectors of both ring laser planes are collinear.

According to the ring laser equation, the relationship between the obtained Sagnac frequency and the input rotation rate is linear over a wide dynamic range. The $M = 7.7$ earthquake near the Fiji Islands on 19 August 2002, was recorded on both ring lasers simultaneously. Figure 29.5 shows the first 15 seconds of this earthquake. The measured raw Sagnac frequency as a function of time was converted to rotation rate in nanoradians per second using Eq. (29.1). Apart from this conversion the data has not

been modified. The dataset from the C-II ring laser is much more noisy than the data from UG1, because there is almost a factor of 20 difference in the respective scale factors. Nevertheless one can see that both ring lasers measure exactly the same signal in phase as well as in amplitude. It has to be stressed again that apart from the unit conversion, the comparison in Fig. 29.5 uses raw data only.

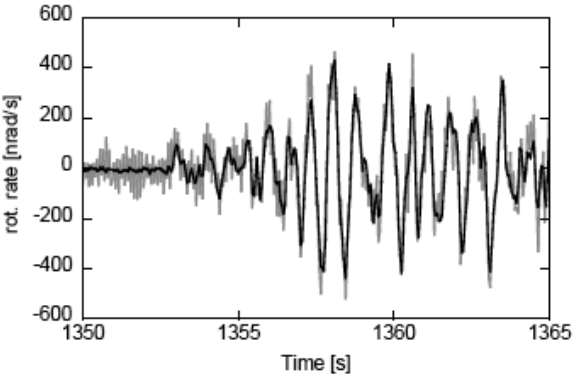

Fig. 29.5 Comparison of two ring laser seismograms from the same $M = 7.7$ earthquake near Fiji on 19 August 2002. Both ring lasers were located in the same place with identical orientation. Apart from the higher noise level of the smaller instrument the recordings are identical

29.2.4 Detection properties

Ring lasers provide optical interferograms where the external rate of rotation is proportional to the rate of change of the fringe pattern. This signal becomes available as an audio-frequency at the output of a photomultiplier tube. In seismology it is important to detect the rate of change of this frequency at 50 ms intervals (20 Hz) very accurately. Since frequency counting techniques do not provide a sufficient resolution at such short averaging intervals, a frequency demodulation concept has been developed. A voltage controlled oscillator is phase locked to the Sagnac frequency of the ring laser, exploiting the fact that Earth rotation provides a constant rate bias in the absence of any seismically induced rotation signals. In the event of an earthquake, one obtains the rate of change of the Sagnac frequency at the feedback line of the voltage controlled oscillator. This voltage can be digitized and averaged at the required 20 Hz rate or higher. Currently, the upper limit for the detectable rate of change from a large ring laser is not set by the rotation sensor itself but by the frequency extraction process.

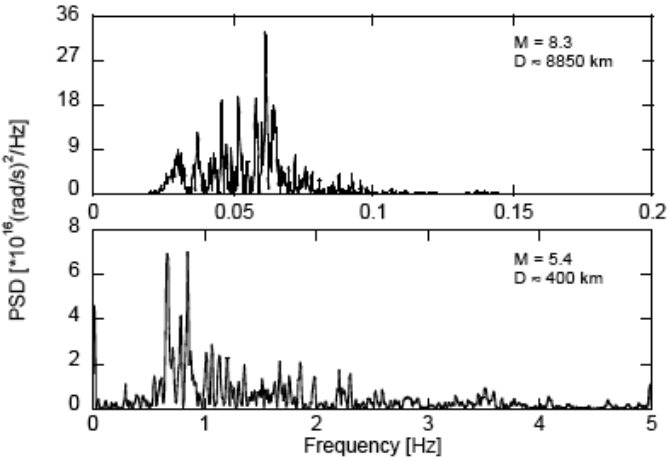

Fig. 29.6 Comparison of recorded rotation spectra from an teleseismic event (Hokkaido: 9 September 2003) and a regional earthquake (France: 22 February 2003). The much higher bandwidth of the rotational wave spectra requires alternative data acquisition techniques such as the demodulator

To outline the importance of the frequency demodulation technique two earthquakes with distinctly different properties are compared. Figure 29.6 shows an example for a teleseismic event and an example from a much closer regional earthquake. While for the remote earthquake the spectral power density essentially drops off to zero above frequencies of 0.1 Hz, one can still see some signal signature up to about 4 Hz for the regional event. Frequencies with a rate of change above 2 Hz, however, are already outside the regime of reliable representation in phase and amplitude by conventional frequency counting and second order autoregression frequency analysis (McLeod et al. 2001).

29.3 Detection of Seismic Signals

For example, the 4×4 m^2 ring laser G installed in the Geodetic Observatory Wettzell has a sensor resolution of $\delta\varphi = 9\times10^{-11}\,\mathrm{rad/s^{1/2}}$. This outstanding sensitivity is appropriate for the detection of both teleseismic waves and near source seismic signals. Typical seismic signals require a high sensor stability for up to one hour of continuous data acquisition. This requirement is much reduced as compared to the long-term stability necessity of the instrument G for the geodetic applications for which it has been built.

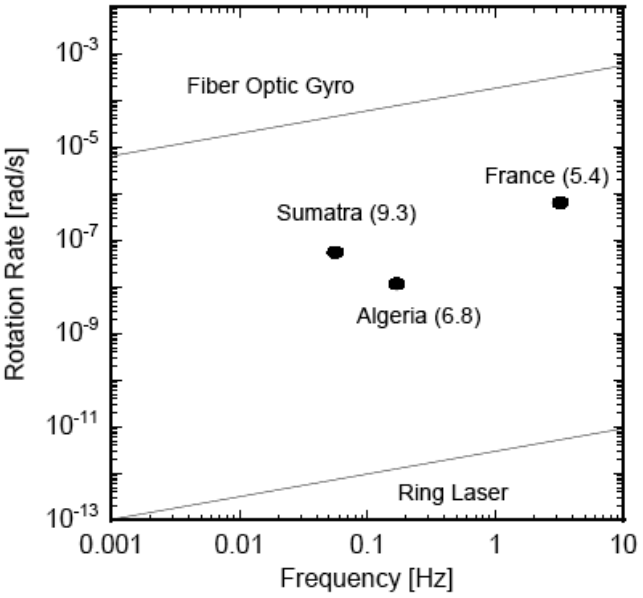

Fig. 29.7 Sensor resolution of different rotation sensor concepts in relation to the observed signal strength of some earthquakes at different epicentral distances

Figure 29.7 illustrates some basic characteristics for the detection of rotations from seismic signals. The diagram shows most of the measurement range of interest for seismic studies. The relevant frequency window is plotted horizontally, while the magnitude of the respective rotation rates is displayed on the vertical. In order to keep this diagram simple the strong motion region is not shown. In the lower part of the plot one can see a line which indicates the resolution limit for current ring lasers. Depending on the actual scale factor, the sensitivity differs from one ring laser to another. However, within the *y*-scale of this chart this line gives a good representation for the existing large ring lasers in general. The current high quality fiber optic gyros (FOG) exhibit a sensor resolution $\delta\varphi = 0.1°/\mathrm{h}^{1/2}$ or slightly less. The upper line was derived from test measurements of a sample FOG type instrument: μFORS-1 manufactured by LITEF in Germany. Both lines are sloping over the frequency range of interest. This reflects the improvement resulting from longer integration as the frequency of interest reduces. To give an idea of the real sensor requirement, three very different examples of earthquakes are indicated on the graph. The details of these earthquakes are given in Table 29.1. Since the Earth crust acts as a lowpass filter one can see that the earthquakes at the right side of the Fig. 29.7 plot are the closest.

Table 29.1 Details of some earthquakes recorded in Germany

Source	Magnitude	Distance [km]
Sumatra	9.3	> 10000
Algeria	6.8	1550
France	5.4	400

All events listed here produced datasets with good signal to noise ratio on the G ring laser. Figure 29.8 shows a raw dataset as an example.

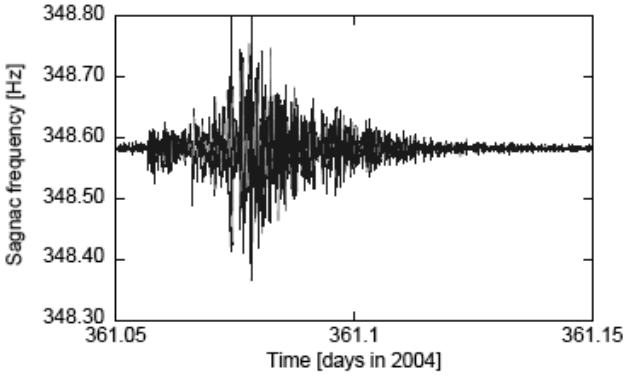

Fig. 29.8 The raw rotation measurement of the $M = 9.3$ Sumatra earthquake from 26 December 2004. The dataset was recorded with a good signal to noise ratio

None of these events would have been within the sensor resolution of FOG. As clearly seen in Fig. 29.7, the application of FOGs for seismic studies is currently possible only for strong motion applications.

29.4 GEOsensor

Based on the discussion of the previous sections one can formulate a concept for a sensitive seismic rotation sensor. In order to obtain a stable interferogram of the two laser beams, the cavity length has to be kept constant to within a fraction of a wavelength. Therefore, usually ring laser bodies are made from Zerodur, a glass ceramic which exhibits a very small relative thermal expansion of $\alpha = 5 \times 10^{-8}$ per K. Since a ring laser for seismic applications requires an enclosed area of more than 1 m^2, a monolithic ring construction would be both too expensive and not transportable.

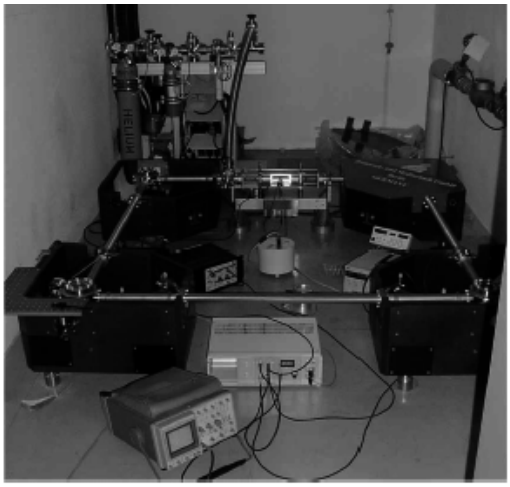

Fig. 29.9 Photo of the GEOsensor ring laser during sensor integration

Figure 9 shows the actual ring laser hardware. The laser cavity has the shape of a square. The four adjustable mirrors are each located in a solid corner box for maximum mechanical stability. The adjustable mirrors are located inside steel containers which in turn are connected together with stainless steel tubes, forming an evacuated enclosure for the laser beams. In the middle of the far side the steel tubes are reduced to a small glass capillary of 4 mm in diameter and a length of 10 cm, which is required for gain medium excitation. When operated, the ring laser cavity is first evacuated and then filled with a mixture of helium and neon reaching a total gas pressure of approximately 6 hPa. In the background of Fig. 29.9 the vacuum pump and filling station can be seen. Other subsystems like the seismometer, the rf-transmitter and the beampower stabilizer are placed inside the ring laser boundary. The following two important considerations are unique for the GEOsensor design:

- Since the ring laser is constructed from several components, it requires a stable concrete platform base at the location of deployment. Such a pad is simple to specify and can be prepared totally independently of the actual GEOsensor deployment.
- The actual area of the ring laser component is not predetermined by the design. The instrument can be built according to the available space at the host observatory. Different GEOsensor realizations may therefore have different size and consequently different instrumental resolution. The length of the current instrument is 1.6 m on a side, which provides an area of 2.56 m^2.

In order to operate the GEOsensor, the cavity must be evacuated, baked and filled with a He/Ne gas mixture. This procedure requires a turbo molecular pump system and a manifold with a supply of ^{4}He, ^{20}Ne and ^{22}Ne. The pump system is not required during the operation of the GEOsensor, but is necessary for the preparation of the instrument and once or twice a year in order to change the laser gas. Laser excitation itself is achieved via a high frequency generator, matched to a symmetrical high impedance antenna at the gain tube. A feedback loop maintains the level of intensity inside the ring laser and ensures monomode operation. When the ring laser is operated it detects the beat note caused by Earth rotation as a rate bias. The magnitude of this beat frequency depends on $\sin\Phi$, with Φ the latitude of the ring laser location. Table 29.2 shows the value of the Earth's rate bias for a few locations of interest, for the GEOsensor with 1.6 m arms.

Table 29.2 Earth rotation bias for some GEOsensor locations

Location	Frequency [Hz]
Wettzell, Germany (49.145 N)	138
Pinon Flat, CA (33.6 N)	102
Tokyo, Japan (35.4 N)	106
Cashmere, NZ (43.57 S)	127

To date, the GEOsensor has been operated at the first two locations. Since the Earth rotation acts like a rate bias on our ring laser measurements, any rotations caused by earthquakes will show up as a frequency modulation around the measured Earth rate.

Acknowledgement. The combined ring laser results were possible because of a collaboration of Forschungseinrichtung Satellitengeodäsie, Technische Universität München, Germany, University of Canterbury, Christchurch, New Zealand and Bundesamt für Kartographie und Geodäsie, Frankfurt, Germany. The GEOsensor was funded under the programme GEOTECHNOLOGIEN of BMBF and DFG, Grant 03F0325 A-D. The authors would also like to acknowledge the IQN Program by the German Academic Exchange Service and the Leibniz Computing Centre Munich for providing access to their supercomputers. University of Canterbury research grants, contracts of the Marsden Fund of the Royal Society of New Zealand and also grants from the Deutsche Forschungsgemeinschaft (DFG) are gratefully acknowledged.

References

Aronowitz F (1971) The laser gyro. In: Ross M (ed) Laser applications, vol 1. Academic Press, New York, pp 133-200

Aki K, Richards PG (2002) Quantitative Seismology, 2nd ed. University Science Books, Sausalito, CA

Igel H, Schreiber KU, Flaws A, Schuberth B, Velikoseltsev A, Cochard A (2005) Rotational motions induced by the M8.1 Tokachi-oki earthquake, September 25, 2003. Geophys Res Lett **32:** L08309, doi:10.1029/2004GL022336

McLeod DP, Stedman GE, Webb TH, Schreiber KU (1998) Comparison of standard and ring laser rotational seismograms. Bull Seism Soc Amer **88**: 1495-1503

McLeod DP, King BT, Stedman GE, Schreiber KU, Webb TH (2001) Autoregressive analysis for the detection of earthquakes with a ring laser gyroscope. Fluctuations and Noise Letters **1**: 1, R41-R50

Pancha A, Webb TH, Stedman GE, McLeod DP, Schreiber U (2000) Ring laser detection of rotations from teleseismic waves. Geophys Res Lett **27**: 3553-3556

Schreiber U, Schneider M, Rowe CH, Stedman, GE, Schlüter W (2001) Aspects of ring lasers as local earth rotation sensors. Surveys in Geophysics **22**: 5-6, 603-611

Schreiber KU, Stedman GE Klügel T (2003) Earth tide and tilt detection by a ring laser gyroscope. J Geophys Res **108**: B2, 10.1029/2001JB000569

Schreiber KU, Velikoseltsev A, Rothacher M, Klügel T, Stedman GE, Wiltshire DL (2004a) Direct measurement of diurnal polar motion by ring laser gyroscopes. J Geophys Res **109**: B6, 10.1029/2003JB002803, B06405

Schreiber U, Velikoseltsev A, Stedman GE, Hurst RB, Klügel T (2004b) Large ring laser gyros as high resolution sensors for applications in geoscience. Proc. 11th Intern Conf on Integrated Navigation Systems, St. Petersburg, 326-331

Stedman GE (1997) Ring laser tests of fundamental physics and geophysics. Rep Progr Phys **60**: 615-688

Takeo M, Ito HM (1997) What can be learned from rotational motions excited by earthquakes? Geophys J Int **129**:319–329

Trifunac MD, Todorovska MI (2001) A note on the usable dynamic range of accelerographs recording translation. Soil Dyn Earth Eng **21**: 275-286